The Journal of Chemical Physics

Low temperature protein refolding suggested by molecular simulation

Cite as: J. Chem. Phys. **151**, 185101 (2019); https://doi.org/10.1063/1.5128211
Submitted: 17 September 2019 . Accepted: 23 October 2019 . Published Online: 11 November 2019

Daniel J. Kozuch, Frank H. Stillinger, and Pablo G. Debenedetti

AIP Publishing

The Journal of Chemical Physics ARTICLE scitation.org/journal/jcp

Low temperature protein refolding suggested by molecular simulation

Cite as: J. Chem. Phys. 151, 185101 (2019); doi: 10.1063/1.5128211
Submitted: 17 September 2019 • Accepted: 23 October 2019 •
Published Online: 11 November 2019

Daniel J. Kozuch,[1] Frank H. Stillinger,[2] and Pablo G. Debenedetti[1,a)]

AFFILIATIONS

[1]Department of Chemical and Biological Engineering, Princeton University, Princeton, New Jersey 08544, USA
[2]Department of Chemistry, Princeton University, Princeton, New Jersey 08544, USA

[a)]Electronic mail: pdebene@princeton.edu

ABSTRACT

The function of critical biological materials, such as proteins, is intrinsically tied to their structure, and this structure is in turn heavily dependent on the properties of the solvent, most commonly water or dilute aqueous solutions. As water is known to exhibit anomalous properties, especially at supercooled temperatures, it is natural to ask how these properties might impact the thermodynamics of protein folding. To investigate this question, we use molecular simulation to explore the behavior of a model miniprotein, Trp-cage, as low as 70 K below the freezing point of the solvent at ambient pressure. Surprisingly, we find that while the expected cold denaturation of the protein is observed at moderate supercooling, further cooling to more than 55 K below the freezing point leads to cold *refolding* of the protein. Structural and hydrogen bonding analysis suggests that this refolding is driven by the desolvation of the protein's hydrophobic core, likely related to the pronounced decrease in density at this temperature. Beyond their intrinsic fundamental interest, these results have implications for cryomicroscopy and cryopreservation, where biological materials are often transiently subjected to these extreme conditions.

I. INTRODUCTION

Water's anomalous properties upon supercooling, such as its sharply increasing heat capacity[1] and compressibility,[2] have long been of interest to the scientific community, but the homogeneous nucleation of ice has impeded experimental observations at temperatures lower than ~232 K.[3] However, in 2014, Sellberg *et al.*[4] demonstrated that ultrafast x-rays could be used to probe bulk liquid water at the millisecond time scale in evaporatively cooled, micrometer sized droplets at temperatures as low as 227 K, corresponding to a supercooling of 46 K. Subsequent work utilizing a similar approach identified a maximum in water's isothermal compressibility at 229 K,[5] consistent with the hypothesis of a low temperature liquid-liquid critical point at higher pressures.[6] While these investigations of supercooled water are important to our fundamental understanding of water physics, the broader exploration of this substance's behavior in noncrystalline low-temperature states, both liquid and glassy, is also relevant to practical applications such as cryoelectron microscopy[7] and cryopreservation.[8]

As advances in experimental techniques allow access to metastable states at progressively lower temperatures, it is natural to inquire how water's distinctive properties at deeply supercooled conditions may affect the behavior of biomolecules, which are often probed under cryogenic conditions.[9] In this work, we are specifically interested in water's role in protein folding at these temperatures. As the homogeneous nucleation of ice still poses nontrivial experimental challenges, molecular simulation is a valuable complementary tool to investigate these questions, given that the small time and length scales typically involved make ice formation statistically unlikely.[10]

Because of the slow dynamics at low temperatures, advanced sampling techniques are required to properly simulate protein folding in the supercooled region. Work by Yang *et al.* demonstrated that Parallel Tempering (PT),[11,12] also known as Replica Exchange Molecular Dynamics (REMD), can be used to study the cold denaturation of a β-hairpin.[13] Further work by Kim *et al.* used the same technique to measure the folding thermodynamics of the model miniprotein, Trp-cage, down to 210 K[14] (note, however, that this corresponds to a supercooling of only 40 K due to the low melting

temperature[15] of the TIP4P/2005 water model[16] used in that work). Additional studies investigating the protein dynamical transition have explored even lower temperatures,[17,18] but these studies do not attempt to fully sample the folding behavior of proteins or other biomolecules.

In this work, we aim to extend the study of Kim *et al.*[14] to even lower temperatures, probing supercooling exceeding 45 K, where anomalous behavior is more pronounced. We choose to investigate the same system, Trp-cage in TIP4P/2005 water, which is attractive for a number of reasons: (1) Trp-cage is small (20 residues) with a fast folding time (<4 μs),[19] making it computationally efficient to investigate and relevant to cryomicroscopy and cryopreservation applications where even rapid cooling (up to 10^6 K/s)[20] implies liquid sample lifetimes on the way to vitrification more than two orders of magnitude larger than the folding time. (2) Even though Trp-cage is small, it possesses both secondary structure motifs (α-helix and 3_{10}-helix) and the tertiary structure with a hydrophobic core, which mimic larger biologically relevant proteins. (3) TIP4P/2005 is well-known to accurately reproduce many of water's thermodynamic properties and has been the subject of numerous studies in the supercooled region.[16,21–23] (4) When Trp-cage is described by the Amber03w force field[24] in combination with TIP4P/2005 water, good agreement with experimental folding kinetics[25] and thermodynamics[14] is obtained. However, as mentioned above, the low melting temperature of TIP4P/2005 with respect to real water means that to investigate supercooling greater than 45 K, one needs to sample temperatures lower than 205 K. To obtain meaningful results over a significant range of low temperatures, we investigate Trp-cage's folding thermodynamics down to 180 K.

When working at such significant supercooling, it is not only important to consider slow protein dynamics, as mentioned above, but also slow water dynamics. In the simulations of the TIP4P/2005 water model, Abascal and Vega addressed this issue by considering whether the mean squared displacement of water reached a value of the order of the square of the water's molecular diameter (which they took to be 0.08 nm^2) in less than 100 ns.[21] They found that, at ambient pressure, TIP4P/2005 failed to attain that threshold mobility below 190 K. For comparison, we have performed extended molecular dynamics simulations at 180 and 192 K for our protein/water system, and found that water diffuses 0.08 nm^2 in 1.4 μs and 220 ns, respectively (see the supplementary material). We also calculate the density autocorrelation decay times for the 180 K and 192 K systems to be on the order of 100 ns and 20 ns, respectively (see the supplementary material). While these long diffusion/decay times certainly make molecular dynamics sampling difficult, they do not preclude the relaxation of these systems on real time scales, which, even for rapidly quenched samples, are at least on the order of 10^{-4} s prior to vitrification (as discussed above).

As a further check, we also calculate the glass transition temperature (T_g) of TIP4P/2005. Work by Jehser *et al.* placed T_g at 193 K,[26] but this was for high pressure (3000 bars) and rapid cooling (200 K/ns). By measuring ambient pressure T_g at several different cooling rates, we calculate T_g at 10^6 K/s (0.001 K/ns) to be 159 K by extrapolation (see the supplementary material). Our lowest temperature, 180 K, is therefore well above the T_g of TIP4P/2005 that might be observed at experimental cooling rates. This being said, care must be taken when considering results below 200 K. We ensure convergence by comparing results from two sets of simulations with different initial conditions (see Sec. II for more details), but due to the necessary use of advanced sampling techniques, which preclude deterministic molecular motion, it is hard to estimate how long the system would need to relax under standard molecular dynamics in order to observe the low-temperature folding behavior reported in this work.

In order to enable equilibrium sampling at these very low temperatures, we rely on an extended version of PT, known as Parallel Tempering in the Well Tempered Ensemble (PT-WTE).[27] This method is a combination of PT and metadynamics,[28] where a history dependent bias is placed on the potential energy, so as to force the system to uniformly sample its underlying energy landscape. This broadens the potential energy distribution, enhancing sampling and simultaneously decreasing the number of replicas required for PT, therefore significantly increasing the computational efficiency. Because of these benefits, PT-WTE has recently been successfully applied to a number of biological systems.[29–32] Specific details of the implementation are given in Sec. II. The results of our calculations are presented in Sec. III, and the principal conclusions are summarized in Sec. IV.

II. METHODS

All simulations were performed with GROMACS 2016.4.[33–36] The reference structure for Trp-cage was obtained from the PDB Database (www.rcsb.org), PDB ID: 1L2Y. The protein was solvated in an octahedral box containing 2617 water molecules, giving a distance greater than 2 nm between any protein atom and any protein atom in the periodic image, so as to avoid any self-interaction. Charge neutralization was achieved via the addition of a single chloride ion. The protein and water were modeled with the Amber03w[24] and TIP4P/2005[16] force fields, respectively.

The time step was set to 2 fs, and a cutoff of 1 nm was used for short range van der Waals and Coulomb electrostatics. Long range electrostatics were accounted for with the Particle-Mesh-Ewald (PME) method,[37] with a Fourier spacing of 0.12 nm and 4th order interpolation. Protein bonds were constrained using the linear constraint solver algorithm,[38] and the rigidity of the water molecules was maintained via SETTLE.[39] Temperature coupling was performed with the v-rescale thermostat,[40] while pressure coupling was performed with the Berendsen barostat[41] during equilibration for numerical stability and the Parrinello-Rahman barostat[42] during sampling.

Initial folded configurations were prepared by first performing steepest decent energy minimization, followed by equilibration for 1 ns at 300 K. The system was then cooled from 300 K to 180 K at 1 K/ns to produce conformations at all desired temperatures below 300 K. The 300 K configuration was used as the initial configuration for all temperatures above 300 K. Unfolded initial configurations were prepared by heating the equilibrated system to 500 K at 5 K/ns to produce an unfolded state, which was then rapidly cooled at 5 K/ns to 180 K, to produce unfolded initial configurations at each desired temperature. Each unfolded configuration was checked to ensure that it was truly an unfolded state according to the criterion defined in Sec. III.

All sampling was done with PT-WTE[27] using an optimized temperature scheme ranging from 180 K to 500 K according to

the method of Lee and Olson,[43] which places additional replicas near bottleneck regions to decrease round trip times. As a result, exchange probabilities varied from 20% to 80%. The well tempered ensemble (WTE) was sampled by performing metadynamics with the PLUMED plugin version 2.4.1.[44] By definition, the collective variable being biased was the potential energy, with Gaussian bias hills of height 1 placed every 500 steps (1 ps) and a bias factor of 25. Exchanges were attempted every 1000 steps (2 ps) between neighboring replicas, with an average round trip time of 550 ns. The system was run for 4 μs, giving a total simulation time of 112 μs.

Because PT-WTE applies a bias to the system, all results were first properly reweighted.[45] Convergence of the folded and unfolded results was observed after 3 μs. Sampling was performed from 3 to 4 μs, which is more than 10 times longer than the density autocorrelation time calculated at the lowest temperature. Error estimates were obtained by splitting the trajectory from 3 to 4 μs into 10 separate parts and calculating the standard deviation from that set.

We note as a useful reference that sampling with normal PT was also attempted for this study, where 144 replicas were used to sample the same temperature range. However, after 10 μs (a total simulation time of more than 1.4 ms), the system had not converged at the lowest temperatures. Accordingly, those results are not included.

While the formation of ice in molecular simulation is unlikely, it is not impossible. Therefore, we calculated the local average Steinhardt order parameter, $\langle q_6 \rangle$[46] and found that it is always less than 0.5. Since $\langle q_6 \rangle$ should be greater than 0.7 for ice,[47] our systems are always liquid.

All hydrogen bonding statistics were calculated using the GROMACS *hbond* utility. A hydrogen bond is defined as a donor-acceptor distance less than 0.35 nm and a hydrogen-donor-acceptor angle less than 30°.

III. RESULTS AND DISCUSSION

To discuss the folding properties of a protein in simulation, a suitable order parameter must be selected to classify a given structure as folded or unfolded. Following the method of Kim *et al.*,[14] Trp-cage was defined as folded for all C-α RMSD <0.3 nm, where C-α RMSD is the root-mean-squared deviation between a given structure and a reference NMR structure (PDB Code: 1L2Y) for the coordinates of the α carbons. Using this definition, fraction folded curves were calculated from multimicrosecond PT-WTE trajectories initiated from both the folded and unfolded states, shown in Fig. 1. Convergence of results from both trajectories ensures that proper sampling was achieved and that the results are not biased by any initial configuration.

From the mean fraction folded data (f), the free energy (FE) of unfolding was calculated using the following relationship:[14]

$$\Delta G_U = G_U - G_F = -RT \ln\left(\frac{1-f}{f}\right). \quad (1)$$

Shown in Fig. 1, ΔG_U displays the previously observed parabolic behavior from 200 K to 500 K,[14,48–50] with cold and hot unfolding occurring at 224 K and 342 K, respectively. These transitions correspond to the condition $f = 0.5$ or, equivalently,

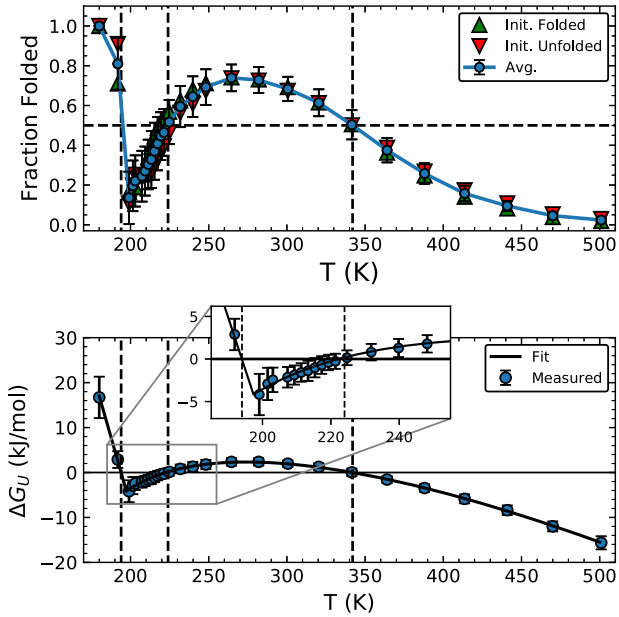

FIG. 1. (top) Fraction folded for the Trp-cage miniprotein as a function of temperature. (bottom) Temperature dependence of the free energy of unfolding as calculated from the fraction folded. The solid line is a piecewise analytic fit. Vertical dashed lines are the cold refolding, cold unfolding, and hot unfolding temperatures at 194 K, 224 K, and 342 K, respectively. Error bars show one standard deviation as calculated from block averaging. The inset in the lower figure highlights the region where replicas were spaced closer together.

$\Delta G_U = 0$. Remarkably, we observe a minimum in the fraction folded curve near 200 K (50 K of supercooling) with the refolding of the protein at 194 K and $f = 1$ at 180 K. This result is quite surprising, and while recent work by Menon and Sengupta noted increased structural persistence in an amyloid oligomer at low temperature,[51] the present study is the first work of which we are aware that demonstrates a sign change in ΔG_U from negative to positive for a protein under supercooled conditions.

In order to visualize the unfolding transitions, structures corresponding to selected C-α RMSD values are shown in Fig. 2. Clearly, heat denaturation results in a totally unstructured loop for the whole chain. On the other hand, cold denaturation is more subtle and mainly characterized by the destabilization of the small 3_{10}-helix at residue 12–14, which is replaced by a less structured and more open loop. However, much of the secondary structure, including the α-helix, is retained.

A more quantitative investigation is performed by studying the distributions for the C-α RMSD and an additional order parameter, W6-S14, defined as the minimum distance between residues 6 and 14. W6-S14 is small for a compact, hydrophobic core and large for a more open, hydrated core.[14,53] The results in Fig. 3 show that cold unfolding at 200 K corresponds to a C-α RMSD between 0.3 and 0.4 nm, with a large W6-S14 distance >0.4 nm. In contrast, cold refolding at 180 K is more similar to the behavior of Trp-cage at 300 K, with a C-α RMSD <0.3 nm, and a W6-S14 distance <0.4 nm.

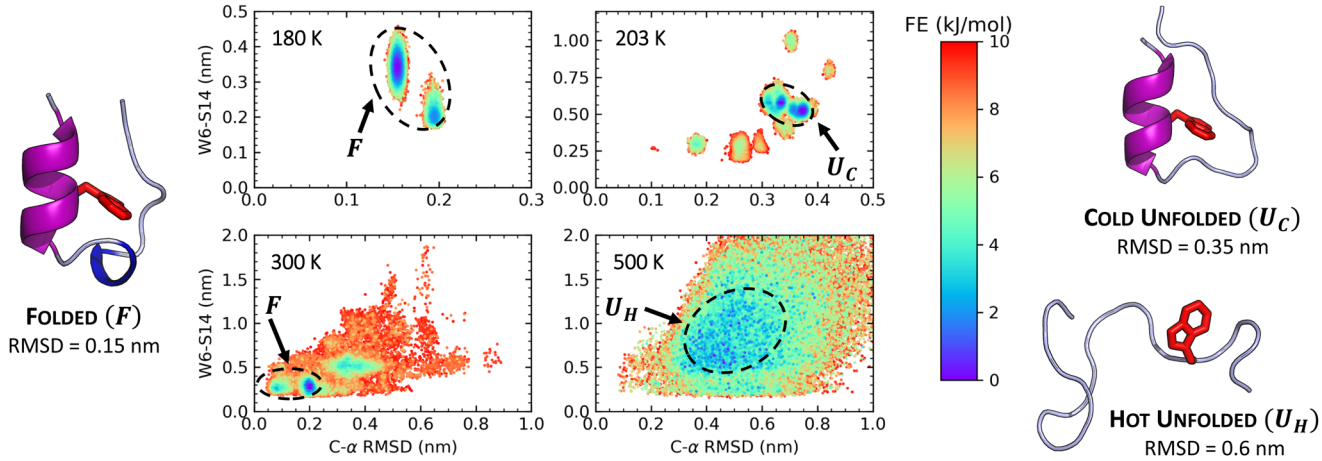

FIG. 2. 2D free energy (FE) maps of C-α RMSD and W6-S14 distance at 180, 203, 300, and 500 K with secondary structure representations of the Trp-cage miniprotein. α-helices are colored in purple, 3_{10}-helix in dark blue, and unstructured segments in gray. The hydrophobic core residue, tryptophan, is also shown (without hydrogens) in red. The schematic shows that upon heating, Trp-cage completely unfolds, while under cooling Trp-cage adopts a moderately expanded structure with the loss of the 3_{10}-helix. Then, upon further cooling from the cold unfolded state to below 194 K, Trp-cage refolds to its original room temperature structure. Visualization done with PyMOL.[52]

This indicates that the cold refolding transition corresponds to a collapse of the core from an open, more solvated state to a compact, less solvated state. Although we stress the similarity between the cold folded state and the ambient temperature folded state, it is clear from Fig. 3 that there are some differences. One example is the presence of two distinct peaks in the C-α RMSD distribution under 0.2 nm for the cold folded system, whereas the ambient temperature folded system possesses only one peak at 0.2 nm and a broad peak at 0.35 nm. Some of the difference is undoubtedly due to higher thermal fluctuations at the warmer temperatures, but further structural characterization will be the subject of future studies.

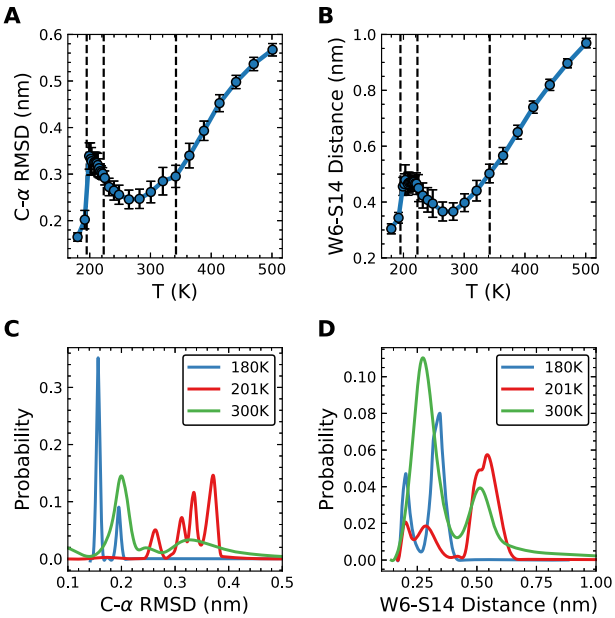

FIG. 3. [(a) and (b)] Mean C-α RMSD and W6-S14 distance as a function of temperature. Vertical dashed lines are the cold refolding, cold unfolding, and hot unfolding temperatures at 194 K, 224 K, and 342 K, respectively. [(c) and (d)] Distribution for C-α RMSD and W6-S14 distance for three selected temperatures: 180 K, 201 K, and 300 K. Error bars show one standard deviation as calculated from block averaging.

The hypothesis of core desolvation driving cold refolding is supported by an investigation of protein-protein (P-P) and protein-water (P-W) hydrogen bonds. Figure 4 shows that the number of P-P hydrogen bonds is minimized in the cold unfolded region, and it increases as the temperature is either raised or lowered. Conversely, the number of P-W hydrogen bonds is maximized in the cold unfolded state, and it decreases with increasing or decreasing temperature. This increase in P-P hydrogen bonding with a simultaneous decrease in P-W hydrogen bonding at temperatures below 200 K corresponds with a more tightly packed, hydrophobic core.

What, then, is driving this cold desolvation? Is a global change in the structure of the solvent (water) responsible? To answer these questions, enthalpic (ΔH_U) and entropic ($T\Delta S_U$) contributions to ΔG_U were calculated, along with the heat capacity of unfolding, $\Delta C_{P,U}$. To do so, we fit ΔG_U with an analytic function, which, due to the limited resolution of data at low temperatures, takes a piecewise form. We note that at the intersection of the two piecewise components (at 197 K), the derivative of ΔG_U is undefined, and as such, we refrain from reporting the relevant quantities at this particular temperature. ΔH_U, ΔS_U, and $\Delta C_{p,U}$ were then calculated using the following relations:

$$\Delta H_U = \left[\frac{\partial(\Delta G_U/T)}{\partial(1/T)}\right]_P, \tag{2}$$

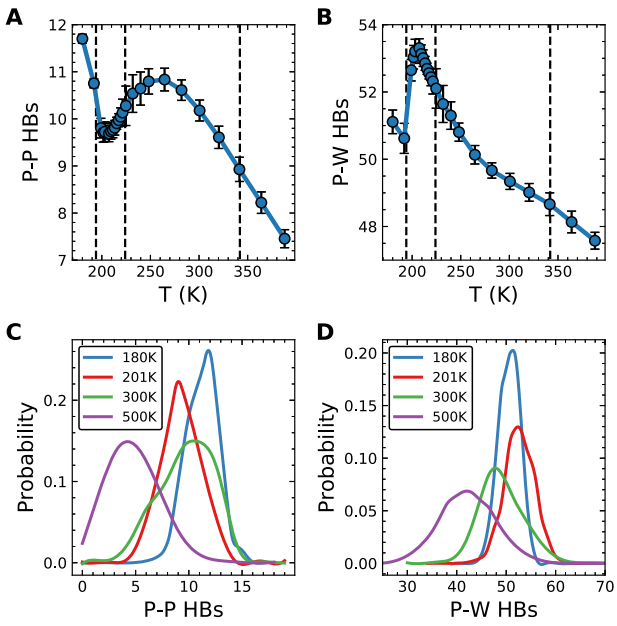

FIG. 4. [(a) and (b)] Mean number of protein-protein (P-P) and protein-water (P-W) hydrogen bonds. Vertical dashed lines are the cold refolding, cold unfolding, and hot unfolding temperatures at 194 K, 224 K, and 342 K, respectively. [(c) and (d)] Distribution of P-P and P-W hydrogen bonds for four selected temperatures: 180 K, 201 K, 300 K, and 500 K. Error bars show one standard deviation as calculated from block averaging.

$$\Delta S_U = -\left[\frac{\partial \Delta G_U}{\partial T}\right]_P, \tag{3}$$

$$\Delta C_{P,U} = \left[\frac{\partial \Delta H_U}{\partial T}\right]_P. \tag{4}$$

The resulting fit of ΔG_U is shown in Fig. 1, and the R^2 coefficient between the measured ΔG_U and the fit ΔG_U was >0.99. Figure 5 shows the results for ΔH_U, $T\Delta S_U$, and $\Delta C_{P,U}$ obtained from Eqs. (2)–(4), respectively.

From this analysis, we observe that ΔH_U and $T\Delta S_U$ become large at the cold refolding temperature, and $\Delta C_{P,U}$ decreases sharply. These results are fully consistent with trends observed for the solvation of a small hydrophobic solute in water as the solvent evolves from higher density at moderately cold temperatures to lower density at low temperatures.[54,55]

The underlying hypothesis, as articulated by Paschek,[55] is that at moderately cold temperatures, the introduction of a hydrophobic solute (such as the solvation of a hydrophobic core) effectively increases the tetrahedral order in the surrounding water, resulting in a negative change in entropy, but also a favorable (negative) change in enthalpy. However, under further supercooled conditions (below 194 K in this work), the water samples are more ordered, low-density configurations where almost all water molecules are tetrahedrally coordinated, even though there is no icelike long-range order. In this

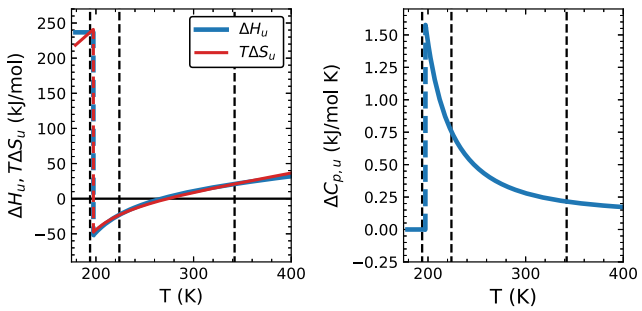

FIG. 5. (left) The enthalpic (ΔH_U) and entropic ($T\Delta S_U$) contributions to the free energy of unfolding (ΔG_U) obtained from Eqs. (2) and (3). (right) Heat capacity of unfolding ($\Delta C_{P,U}$) from Eq. (4). Vertical dashed lines are the cold refolding, cold unfolding, and hot unfolding temperatures at 194 K, 224 K, and 342 K, respectively. Dashed portions of the ΔH_U and $T\Delta S_U$ curves indicate that the value is undefined at this point due to a discontinuity derived from the piecewise fitting of ΔG_U.

environment, the solvation of a hydrophobic solute actually disrupts the existing local order, breaking hydrogen bonds. Accordingly, the change in entropy and enthalpy are both positive, as seen in Fig. 5.

In order to determine whether the system indeed preferentially samples low-density liquid configurations, the density (ρ) and enthalpy (H) were calculated for the total system, as shown in Fig. 6. A density maximum of 1014 kg/m^3 is observed at 282 K, with the density decreasing sharply upon further cooling to 955 kg/m^3 at 180 K. From the perspective of the information theory approach to hydrophobic hydration,[56] a decrease in solvent density facilitates cavity formation and hence should (by itself) favor hydration of small hydrophobic moieties. However, given that TIP4P/2005 water exhibits a maximum in the isothermal compressibility at 230 K at ambient pressure,[23] the decrease in density upon cooling is accompanied by a corresponding decrease in density fluctuations at temperatures below 230 K, which disfavors hydrophobic hydration. Given the fact that Trp-cage's hydrophobic core contains larger aromatic groups that cannot be properly considered as a "small" hydrophobic solute, it is nontrivial to assess quantitatively how this competition between lower density and decreased density fluctuations contributes to the observed refolding behavior.

We also calculate the coefficient of thermal expansion, α_P, and the isobaric heat capacity, C_P, which are defined as follows:

$$\alpha_P = \frac{1}{V}\left[\frac{\partial V}{\partial T}\right]_{N,P}, \quad C_P = \left[\frac{\partial H}{\partial T}\right]_{N,P}. \tag{5}$$

α_P and C_P show peaks near 224 K, consistent with the corresponding volumetric and thermal trends (Fig. 6). Below 194 K, where cold refolding is observed, the decrease in density slows down appreciably, with $\alpha_P \approx 0$. This indicates that we have indeed crossed into the low-density region. Consequently, it is likely that the accompanying transformation in solvent structure plays a significant role in the cold refolding that we observe.

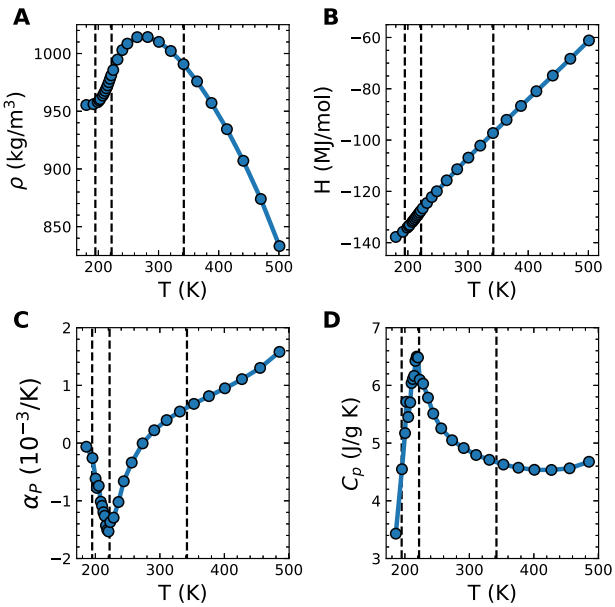

FIG. 6. Thermodynamic properties for the full system. (a) Density, ρ, (b) enthalpy, H, (c) thermal expansion coefficient, α_P, and (d) isobaric heat capacity, C_P. Enthalpy values are in units of energy per mol of the system. Vertical dashed lines are the cold refolding, cold unfolding, and hot unfolding temperatures at 194 K, 224 K, and 342 K, respectively.

IV. CONCLUSION

In this work, we demonstrated that by using a combination of parallel tempering and well-tempered metadynamics, metastable equilibrium folding thermodynamics for a well-solvated model protein, Trp-cage, can be obtained at temperatures as low as 180 K (equivalent to 70 K below bulk freezing for TIP4P/2005 water). Our results show that below 194 K (56 K below freezing), the protein returns to the folded state. Analysis shows that this refolding corresponds to the desolvation of the hydrophobic core, as it becomes more compact and the number of protein-water hydrogen bonds decreases at the lowest sampled temperatures. Additionally, the heat capacity of unfolding, $\Delta C_{P,U}$, decreases sharply at this refolding transition. This decrease in $\Delta C_{P,U}$ occurs at the same temperature at which the surrounding aqueous system finishes evolving from high- to low-density water, leading us to suggest that this striking property of water is the main driver for the protein's low-temperature refolding. Further work is underway to test whether these observations hold for other models of water and other proteins.

SUPPLEMENTARY MATERIAL

See the supplementary material for details regarding the diffusion, density autocorrelation, and glass transition temperature calculations discussed in Sec. I.

ACKNOWLEDGMENTS

P.G.D. gratefully acknowledges support from the National Science Foundation (Award No. CHE-1856704). D.J.K. gratefully acknowledges support from the National Science Foundation (Graduate Research Fellowship Grant No. DGE-1656466).

REFERENCES

[1] C. A. Angell, W. J. Sichina, and M. Oguni, "Heat capacity of water at extremes of supercooling and superheating," J. Phys. Chem. **86**, 998–1002 (1982).
[2] R. J. Speedy and C. A. Angell, "Isothermal compressibility of supercooled water and evidence for a thermodynamic singularity at −45 °C," J. Chem. Phys. **65**, 851–858 (1976).
[3] B. Mason, "The supercooling and nucleation of water," Adv. Phys. **7**, 221–234 (1958).
[4] J. A. Sellberg, C. Huang, T. A. McQueen, N. D. Loh, H. Laksmono, D. Schlesinger, R. G. Sierra, D. Nordlund, C. Y. Hampton, D. Starodub, D. P. DePonte, M. Beye, C. Chen, A. V. Martin, A. Barty, K. T. Wikfeldt, T. M. Weiss, C. Caronna, J. Feldkamp, L. B. Skinner, M. M. Seibert, M. Messerschmidt, G. J. Williams, S. Boutet, L. G. M. Pettersson, M. J. Bogan, and A. Nilsson, "Ultrafast X-ray probing of water structure below the homogeneous ice nucleation temperature," Nature **510**, 381–384 (2014).
[5] K. H. Kim, A. Späh, H. Pathak, F. Perakis, D. Mariedahl, K. Amann-Winkel, J. A. Sellberg, J. H. Lee, S. Kim, J. Park, K. H. Nam, T. Katayama, and A. Nilsson, "Maxima in the thermodynamic response and correlation functions of deeply supercooled water," Science **358**, 1589–1593 (2017).
[6] J. C. Palmer, F. Martelli, Y. Liu, R. Car, A. Z. Panagiotopoulos, and P. G. Debenedetti, "Metastable liquid–liquid transition in a molecular model of water," Nature **510**, 385–388 (2014).
[7] P. Chlanda and M. Sachse, "Cryo-electron microscopy of vitreous sections," Methods Mol. Biol. **1117**, 193–214 (2014).
[8] Y. C. Song, B. S. Khirabadi, F. Lightfoot, K. G. Brockbank, and M. J. Taylor, "Vitreous cryopreservation maintains the function of vascular grafts," Nat. Biotechnol. **18**, 296–299 (2000).
[9] Y. Cheng, N. Grigorieff, P. A. Penczek, and T. Walz, "A primer to single-particle cryo-electron microscopy," Cell **161**, 438–449 (2015).
[10] A. Haji-Akbari and P. G. Debenedetti, "Direct calculation of ice homogeneous nucleation rate for a molecular model of water," Proc. Natl. Acad. Sci. U. S. A. **112**, 10582–10588 (2015).
[11] R. H. Swendsen and J.-S. Wang, "Replica Monte Carlo simulation of spin-glasses," Phys. Rev. Lett. **57**, 2607–2609 (1986).
[12] D. J. Earl and M. W. Deem, "Parallel tempering: Theory, applications, and new perspectives," Phys. Chem. Chem. Phys. **7**, 3910–3916 (2005).
[13] C. Yang, S. Jang, and Y. Pak, "A fully atomistic computer simulation study of cold denaturation of a β-hairpin," Nat. Commun. **5**, 5773 (2014).
[14] S. B. Kim, J. C. Palmer, and P. G. Debenedetti, "Computational investigation of cold denaturation in the Trp-cage miniprotein," Proc. Natl. Acad. Sci. U. S. A. **113**, 8991–8996 (2016).
[15] R. García Fernández, J. L. F. Abascal, and C. Vega, "The melting point of ice Ih for common water models calculated from direct coexistence of the solid-liquid interface," J. Chem. Phys. **124**, 144506 (2006).
[16] J. L. F. Abascal and C. Vega, "A general purpose model for the condensed phases of water: TIP4P/2005," J. Chem. Phys. **123**, 234505 (2005).
[17] M.-C. C. Bellissent-Funel, A. Hassanali, M. Havenith, R. Henchman, P. Pohl, F. Sterpone, D. van der Spoel, Y. Xu, and A. E. Garcia, "Water determines the structure and dynamics of proteins," Chem. Rev. **116**, 7673–7697 (2016).
[18] S. B. Kim, D. R. Gupta, and P. G. Debenedetti, "Computational investigation of dynamical transitions in Trp-cage miniprotein powders," Sci. Rep. **6**, 25612 (2016).
[19] L. Qiu, S. A. Pabit, A. E. Roitberg, and S. J. Hagen, "Smaller and faster: The 20-residue Trp-cage protein folds in 4 μs," J. Am. Chem. Soc. **124**(44), 12952–12953 (2002).
[20] R. F. Thompson, M. Walker, C. A. Siebert, S. P. Muench, and N. A. Ranson, "An introduction to sample preparation and imaging by cryo-electron microscopy for structural biology," Methods **100**, 3–15 (2016).
[21] J. L. F. Abascal and C. Vega, "Widom line and the liquid–liquid critical point for the TIP4P/2005 water model," J. Chem. Phys. **133**, 234502 (2010).

[22]R. S. Singh, J. W. Biddle, P. G. Debenedetti, and M. A. Anisimov, "Two-state thermodynamics and the possibility of a liquid-liquid phase transition in supercooled TIP4P/2005 water," J. Chem. Phys. **144**(14), 144504 (2016).
[23]J. W. Biddle, R. S. Singh, E. M. Sparano, F. Ricci, M. A. González, C. Valeriani, J. L. F. Abascal, P. G. Debenedetti, M. A. Anisimov, and F. Caupin, "Two-structure thermodynamics for the TIP4P/2005 model of water covering supercooled and deeply stretched regions," J. Chem. Phys. **146**, 034502 (2017).
[24]R. B. Best and J. Mittal, "Protein simulations with an optimized water model: Cooperative helix formation and temperature-induced unfolded state collapse," J. Phys. Chem. B **114**, 14916–14923 (2010).
[25]S. B. Kim, C. J. Dsilva, I. G. Kevrekidis, and P. G. Debenedetti, "Systematic characterization of protein folding pathways using diffusion maps: Application to Trp-cage miniprotein," J. Chem. Phys. **142**(8), 085101 (2015).
[26]M. Jehser, M. Seidl, C. Rauer, T. Loerting, and G. Zifferer, "Simulation of high-density water: Its glass transition for various water models," J. Chem. Phys. **140**, 134504 (2014).
[27]M. Bonomi and M. Parrinello, "Enhanced sampling in the well-tempered ensemble," Phys. Rev. Lett. **104**, 190601 (2010).
[28]A. Laio and M. Parrinello, "Escaping free-energy minima," Proc. Natl. Acad. Sci. U. S. A. **99**, 12562–12566 (2002).
[29]F. Palazzesi, M. K. Prakash, M. Bonomi, and A. Barducci, "Accuracy of current all-atom force-fields in modeling protein disordered states," J. Chem. Theory Comput. **11**, 2–7 (2015).
[30]A. Mafi, S. Abbina, M. T. Kalathottukaren, J. H. Morrissey, C. Haynes, J. N. Kizhakkedathu, J. Pfaendtner, and K. C. Chou, "Design of polyphosphate inhibitors: A molecular dynamics investigation on polyethylene glycol-linked cationic binding groups," Biomacromolecules **19**, 1358–1367 (2018).
[31]G. H. Zerze, M. N. Khan, F. H. Stillinger, and P. G. Debenedetti, "Computational investigation of the effect of backbone chiral inversions on polypeptide structure," J. Phys. Chem. B **122**, 6357–6363 (2018).
[32]S. Haldar, F. Comitani, G. Saladino, C. Woods, M. W. van der Kamp, A. J. Mulholland, and F. L. Gervasio, "A multiscale simulation approach to modeling drug–protein binding kinetics," J. Chem. Theory Comput. **14**, 6093–6101 (2018).
[33]B. Hess, C. Kutzner, D. van der Spoel, and E. Lindahl, "GROMACS 4: Algorithms for highly efficient, load-balanced, and scalable molecular simulation," J. Chem. Theory Comput. **4**, 435–447 (2008).
[34]S. Pronk, S. Páll, R. Schulz, P. Larsson, P. Bjelkmar, R. Apostolov, M. R. Shirts, J. C. Smith, P. M. Kasson, D. van der Spoel, B. Hess, and E. Lindahl, "GROMACS 4.5: A high-throughput and highly parallel open source molecular simulation toolkit," Bioinformatics **29**, 845–854 (2013).
[35]S. Páll, M. J. Abraham, C. Kutzner, B. Hess, and E. Lindahl, "Tackling exascale software challenges in molecular dynamics simulations with GROMACS," Solv. Software Challenges Exascale **8759**, 3–27 (2015).
[36]M. J. Abraham, T. Murtola, R. Schulz, S. Páll, J. C. Smith, B. Hess, and E. Lindahl, "GROMACS: High performance molecular simulations through multi-level parallelism from laptops to supercomputers," SoftwareX **1-2**, 19–25 (2015).
[37]U. Essmann, L. Perera, M. L. Berkowitz, T. Darden, H. Lee, and L. G. Pedersen, "A smooth particle mesh Ewald method," J. Chem. Phys. **103**, 8577–8593 (1995).
[38]B. Hess, H. Bekker, H. J. C. Berendsen, and J. G. E. M. Fraaije, "LINCS: A linear constraint solver for molecular simulations," J. Comput. Chem. **18**, 1463–1472 (1997).
[39]S. Miyamoto and P. A. Kollman, "Settle: An analytical version of the SHAKE and RATTLE algorithm for rigid water models," J. Comput. Chem. **13**, 952–962 (1992).
[40]G. Bussi, D. Donadio, and M. Parrinello, "Canonical sampling through velocity-rescaling," J. Chem. Phys. **126**, 014101 (2008).
[41]H. J. C. Berendsen, J. P. M. Postma, W. F. van Gunsteren, A. DiNola, and J. R. Haak, "Molecular dynamics with coupling to an external bath," J. Chem. Phys. **81**, 3684–3690 (1984).
[42]M. Parrinello and A. Rahman, "Polymorphic transitions in single crystals: A new molecular dynamics method," J. Appl. Phys. **52**, 7182–7190 (1981).
[43]M. S. Lee and M. A. Olson, "Comparison of two adaptive temperature-based replica exchange methods applied to a sharp phase transition of protein unfolding-folding," J. Chem. Phys. **134**, 244111 (2011).
[44]G. A. Tribello, M. Bonomi, D. Branduardi, C. Camilloni, and G. Bussi, "PLUMED 2: New feathers for an old bird," Comput. Phys. Commun. **185**, 604–613 (2014).
[45]P. Tiwary and M. Parrinello, "A time-independent free energy estimator for metadynamics," J. Phys. Chem. B **119**, 736–742 (2015).
[46]P. J. Steinhardt, D. R. Nelson, and M. Ronchetti, "Bond-orientational order in liquids and glasses," Phys. Rev. B **28**, 784–805 (1983).
[47]A. Reinhardt, J. P. K. Doye, E. G. Noya, and C. Vega, "Local order parameters for use in driving homogeneous ice nucleation with all-atom models of water," J. Chem. Phys. **137**, 194504 (2012).
[48]V. Bianco and G. Franzese, "Contribution of water to pressure and cold denaturation of proteins," Phys. Rev. Lett. **115**(10), 108101 (2015).
[49]V. Bianco, N. Pagès-Gelabert, I. Coluzza, and G. Franzese, "How the stability of a folded protein depends on interfacial water properties and residue-residue interactions," J. Mol. Liq. **245**, 129–139 (2017).
[50]B. Uralcan and P. G. Debenedetti, "Computational investigation of the effect of pressure on protein stability," J. Phys. Chem. Lett. **10**, 1894–1899 (2019).
[51]S. Menon and N. Sengupta, "The cold thermal response of an amyloid oligomer differs from typical globular protein cold denaturation," J. Phys. Chem. Lett. **10**, 2453–2457 (2019).
[52]L. Schrödinger, The PyMOL Molecular Graphics System, Version 1.8, 2015.
[53]B. Uralcan, S. B. Kim, C. E. Markwalter, R. K. Prud'homme, and P. G. Debenedetti, "A computational study of the ionic liquid-induced destabilization of the miniprotein Trp-cage," J. Phys. Chem. B **122**, 5707 (2018).
[54]N. T. Southall, K. A. Dill, and A. D. J. Haymet, "A view of the hydrophobic effect," J. Phys. Chem. B **106**, 521–533 (2002).
[55]D. Paschek, "How the liquid-liquid transition affects hydrophobic hydration in deeply supercooled water," Phys. Rev. Lett. **94**, 217802 (2005).
[56]G. Hummer, S. Garde, A. E. Garcia, A. Pohorille, and L. R. Pratt, "An information theory model of hydrophobic interactions," Proc. Natl. Acad. Sci. U. S. A. **93**, 8951–8955 (1996).